Comparative Biochemistry and Physiology, Part B 248–249 (2020) 110469

Contents lists available at ScienceDirect

Comparative Biochemistry and Physiology, Part B

journal homepage: www.elsevier.com/locate/cbpb

A potential role for hyperpolarization-activated cyclic nucleotide-gated sodium/potassium channels (HCNs) in teleost acid-base and ammonia regulation

Sandra Fehsenfeld[a,b,*], Chris M. Wood[b]

[a] Université du Quebec à Rimouski, Département de biologie, chimie et géographie, 300 Allée des Ursulines, Rimouski, QC G5L 3A1, Canada
[b] University of British Columbia, Department of Zoology, 4200 - 6270 University Blvd., Vancouver, BC V6T 1Z4, Canada

ARTICLE INFO

Keywords:
High environmental ammonia
Feeding
Kidney
Gill
Brain
Rhesus glycoprotein
mRNA expression
qPCR
Phylogeny

ABSTRACT

Increasing evidence suggests the involvement of hyperpolarization-activated cyclic nucleotide-gated sodium/potassium channels (HCNs) not only in cardiac and neural function, but also in more general physiological processes including acid-base and ammonia regulation. We have identified four different HCN paralogs/isoforms in the goldfish *Carassius auratus* (CaHCN1, CaHCN2b, CaHCN4a and CaHCN4b) as likely candidates to contribute to renal, branchial and intestinal acid-base and ammonia regulation in this teleost. Quantitative real-time PCR showed not only high mRNA abundance of all isoforms in heart and brain, but also detectable levels (particularly of CaHCN2b and CaHCN4b) in non-excitable tissues, including gills and kidneys. In response to an internal or external acid-base and/or ammonia disturbance caused by feeding or high environmental ammonia, respectively, we observed differential and tissue-specific changes in mRNA abundance of all isoforms except CaHCN4b. Furthermore, our data suggest that the functions of specific HCN channels are supplemented by certain Rhesus glycoprotein functions to help in the protection of tissues from elevated ammonia levels, or as potential direct routes for ammonia transport in gills, kidney, and gut. The present results indicate important individual roles for each HCN isoform in response to acid-base and ammonia disturbances.

1. Introduction

Hyperpolarization-activated cyclic nucleotide-gated sodium/potassium channels (HCNs) belong to the voltage-gated cation channel superfamily and are integral membrane proteins that contribute to the generation of membrane potentials in excitable and non-excitable cells (Jackson et al., 2007). In mammals, the four different isoforms / paralogs (HCN1 to HCN4) have been identified to be very similar in their structure: Four subunits are believed to form a tetramer around a core with each subunit containing 6 transmembrane domains hosting a voltage sensor domain in segment 4 and a cation conducting pore between segments 5 and 6 (Jackson et al., 2007). Despite their structural similarities, HCNs can be distinguished by their different quantitative electrochemical properties including voltage-dependence, activation/deactivation kinetics and sensitivity to the nucleotide cyclic AMP (cAMP)(Biel et al., 2009; Santoro and Tibbs, 1990). HCNs contribute to the generation of a current commonly referred to as the "funny" current I_f or I_h. With a Nernst potential of -20 mV, I_f/I_h is inwardly directed at rest and depolarizes the cellular membrane potential. In contrast to being activated upon membrane depolarization like the majority of

Abbreviation: α, the likelihood that the true population parameter lies outside the confidence interval; BLASTn / x, **B**asic **L**ocal **A**lignment **S**earch **T**ool, n = nucleotide – nucleotide, x = translated nucleotide - protein; bp, base pairs; Ca, *Carassius auratus*; cDNA, **c**omplementary **D**eoxyribo**N**ucleic **A**cid; E, expect value, as the number of expected hits of similar quality (score) that could be found just by chance in BLAST analysis; EF1α, Elongation factor 1 alpha; EMBL, **E**uropean **M**olecular **B**iology **L**aboratories; $+G$, discrete gamma distribution for modelling phylogeny; HEA, high environmental ammonia; HCN, hyperpolarization-activated cyclic nucleotide-gated sodium/potassium channels; JTT, **J**ones-**T**aylor-**T**hornton matrix-based model for phylogenetic analyses; k, number of multiple comparisons in statistical analyses; MEGAX, **M**olecular **E**volutionary **G**enetics **A**nalysis, version X (software); mRNA, **m**essenger **R**ibo**N**ucleic **A**cid; MUSCLE, **MU**ltiple **S**equence **C**omparison by **L**og-**E**xpectation, software for multiple sequence alignments; NCBI, **N**ational **C**enter for **B**iotechnology **I**nformation; NKA, Na^+/K^+-ATPase; PAST, **PA**leontological **ST**atistics software package for education and data analysis; qPCR, **q**uantitative real-time **P**olymerase **C**hain **R**eaction; Rhcg / Rhbg, Rhesus glycoprotein isoform cg / bg

* Corresponding author at: Université du Quebec à Rimouski, Département de biologie, chimie et géographie, 300 Allée des Ursulines, Rimouski, QC G5L 3A1, Canada.
E-mail address: Sandra.Fehsenfeld@uqar.ca (S. Fehsenfeld).

https://doi.org/10.1016/j.cbpb.2020.110469
Received 11 May 2020; Received in revised form 24 June 2020; Accepted 2 July 2020
Available online 10 July 2020

cellular conductances, I_f / I_h is rather activated by hyperpolarization to membrane potentials more negative than −55 mV (Biel et al., 2009). HCNs in fishes exhibit very similar properties to the mammalian HCNs, however, they are present in multiple isoforms which likely arose from the most ancestral HCN3 during gene duplication events (Jackson et al., 2007).

Predominantly, HCNs are known to contribute to the spontaneous beating in pacemaker cells and hence for their role in cardiac pacemaking, and/or as key participants in nerve signal transduction, in both mammals (Biel et al., 2009) and fishes (Hassinen et al., 2017; Jackson et al., 2007; Sutcliff et al., 2020; Wilson et al., 2013). Carrisoza-Gaytán and colleagues (Carrisoza-Gaytán et al., 2011), however, discovered that HCN2 in the rat was also involved in renal acid-base regulation by promoting NH_4^+ transport, specifically in acid-secreting intercalated cells in the distal nephron. Furthermore, an HCN channel has been implicated in branchial acid-base regulation in the green crab, *Carcinus maenas*. HCN in this crab also appears to promote transport of NH_4^+, probably by substitution of NH_4^+ for K^+ due to its almost identical size and charge (Fehsenfeld and Weihrauch, 2016; Towle and Holleland, 1987). This leaves fish as particularly interesting study animals, especially for HCN2, as they possess both gills and kidneys that are involved in acid-base and ammonia regulation to different extents under different physiological circumstances (Fehsenfeld et al., 2019; Fehsenfeld and Wood, 2018; Perry and Gilmour, 2006; Wright and Wood, 2012).

As multiple isoforms and paralogs of HCNs are present in other teleosts (Jackson et al., 2007), we hypothesized here that (1) different isoforms of HCNs in the goldfish (*Carassius auratus*) would be differentially expressed in excretory organs and especially in gills and kidney, and (2) acid-base and ammonia disturbances would result in significant changes in mRNA abundance of these isoforms. In order to test our hypotheses, we partially cloned HCN paralogs initially identified in the *Cyprinus carpio* transcriptome and later verified in the goldfish genome using known mammalian and other teleost sequences. We then used quantitative real-time PCR (qPCR) to assess their mRNA abundance in response to challenges of acid-base/ammonia homeostasis by feeding (which induces a postprandial "acidic tide" as well as an ammonia load in agastric fish such as goldfish; Fehsenfeld and Wood, 2018; Wood, 2019; Wood et al., 2010) and exposure to high environmental ammonia. We also checked for simultaneous changes in the mRNA expression of Rhesus glycoproteins (ammonia channels) which are known to be sensitive to these treatments in gills and kidney (e.g. Fehsenfeld and Wood, 2018; Nawata et al., 2007; Sinha et al., 2013; Zhang et al., 2015; Zimmer et al., 2010).

2. Materials and methods

2.1. Animal care

Goldfish *C. auratus* with an approximate length of ~5 cm (2.3 ± 0.1 g, mean ± SE, $N = 18$) were obtained from Noah's Pet Ark (Vancouver, BC, Canada) and kept in recirculating and filtered 75-L aquaria in dechlorinated Vancouver tap water [in μmol/L: ~70 Na^+, 73 Cl^-, 7 Mg^{2+}, 89 Ca^{2+}, pH 6.94 ± 0.03] at 20 °C at a light cycle of 12:12-h light-dark at a maximum density of 1 animal/3 L. Water ammonia and pH levels were closely monitored, and water changes were performed 1–2 times per week as necessary. All fish were fed 3 times/week at 1% of their body weight with commercial flaked food (Nutrafin Max, Hagen, Montreal, QC, Canada).

For experiments, goldfish were either (i) fasted for 96 h ("fasted"), or (ii) fasted for 93 h, then fed to satiation, and sacrificed at 96 h after 3 additional hours for meal processing ("fed"), or (iii) fasted for 48 h and then exposed to 2 mmol L^{-1} NH_4HCO_3 for additional 48 h while still fasting ("fasted/HEA"), then sacrificed at 96 h. For HEA exposure, goldfish were transferred into aerated and darkened individual plastic containers (2 L) enriched with 2 mmol L^{-1} NH_4HCO_3 (nominal concentration). During the experimental period, water changes were performed accordingly every 24 h in all experimental groups (i), (ii) and (iii) to minimize its potential effect as a confounding variable. Water ammonia levels were measured by the salicylate/hypochlorite method (Verdouw et al., 1978) after each fresh addition of NH_4HCO_3 (AMM_{START}) and after 24 h just before water exchanges (AMM_{END}). Whole animal total ammonia excretion was calculated based on these values as AMM_{TOT} = (AMM_{END} - AMM_{START}) / 24 h / g in order to evaluate whether goldfish could still excrete ammonia against this high outside concentration.

Each animal was quickly killed by cephalic concussion to avoid potential effects of anaesthetics. Brain and heart (hereafter referred to as "excitable organs" being composed of predominantly excitable tissue), as well as kidney, gill, gut and liver (hereafter referred to as "non-excitable organs" due to the predominance of other tissue types over contributing excitable tissue) were harvested and immediately transferred into RNAlater® (Sigma-Aldrich, Darmstadt, Germany), incubated at 4 °C over night, and then stored at −80 °C until RNA isolation (see below). All procedures were conducted under the approval of the University of British Columbia Animal Care and Use Committee (A14–0251) and the guidelines of the Canadian Council on Animal Care.

2.2. Identification of candidate HCNs and quantitative real-time PCR (qPCR)

Sequences for HCN1–4 (and isoforms, where available – see Supplemental Table 1) from *Homo sapiens*, *Rattus norvegicus*, *Mus musculus* and diverse fish species including zebrafish *Danio rerio*, rainbow trout *Oncorhynchus mykiss*, Atlantic salmon *Salmo salar*, and Japanese pufferfish *Takifugu rubripes*, were used to screen the transcriptome of *Cyprinus carpio* (as at the start of the study the goldfish genome was not readily available) to identify potential HCN candidate genes. Primers for the respective HCN isoforms in *C. auratus* (CaHCN) were designed based on these *Cyprinus carpio* sequences. The PCR products from this initial identification step were designed to result in 300–400 bp amplicons and these were then sequenced.

For qPCR experiments, nested primers on the obtained CaHCN fragments resulting in ca. 100 bp amplicons were designed and tested for specificity and efficiency (see below). Primers for Rhesus glycoproteins were used as established in earlier studies (Lawrence et al., 2015; Sinha et al., 2013). The mRNAs of all tissues and treatments (stored in RNAlater® (Ambion) at −80 °C) were isolated under RNase-free conditions using Trizol (Invitrogen, Carlsbad, CA, USA). After treatment with DN*ase* I (Invitrogen, Carlsbad, CA, USA), mRNA was quantified by NanoDrop™ analysis (2000c Spectrophotometer, Thermo Fisher Scientific, Waltham, MA, USA) and tested by regular PCR to ensure that no DNA contamination was present. Subsequently, 0.9 mg of clean mRNA was reverse transcribed into cDNA using the iScript cDNA synthesis kit (Bio-Rad, Mississauga, ON, Canada) and again tested by regular PCR to ensure success of the transcription. Each qPCR reaction (15 μL) was set up with 0.4 pmol primer, 2 μL cDNA and 7.5 μL SSO FastEvaGreen Supermix (Bio-Rad). All reactions were run in 96-well plates on a Bio-Rad CFX connect cycler and analysed with the Bio-Rad CFX manager 3.1 software (Mississauga, ON, Canada). Each run included a cDNA denaturation step (2 min at 98 °C), followed by 40 cycles of 5 s at 98 °C and 20 s at 60 °C for annealing. A melt curve analysis from 65 °C to 95 °C in 1 °C increments was run to verify single amplicons. A standard curve based on a 1:1 serial dilution of a cDNA-mix of all tissues of interest was included to quantify mRNA expression and to determine primer efficiency for each gene (see Supplemental Table 2 for details on primers). To normalize mRNA abundance, the geometric mean of β-actin and elongation factor 1 α mRNA expression (BA*Ef1α) was used after being identified for best suitability using Normfinder (Andersen et al., 2004) and also checked to not exhibit any significant change in mRNA abundance among treatments (ANOVA with $P > .14$).

2.3. Phylogenetic analysis

All sequences that were used to identify initial candidates for HCN in *C. carpio / C. auratus* were included in the phylogenetic analysis as listed in Supplementary Table 1. All protein sequences of the respective genes were aligned with MUSCLE in MEGA X (Kumar et al., 2018) with the default parameter settings. Subsequently, the testing function was used to identify the best fitting model to calculate the phylogenetic tree.

When the goldfish genome became available (NCBI *Carassius auratus* Annotation Release 100, **BioProject PRJNA481500**), only the mammalian HCNs were blasted against it in the NCBI database, resulting in up to 100 hits for each HCN including repetitive, fragmented and partial sequences. To eliminate truncated and repetitive sequences, only hits with an Expect value E = 0.00 that were not fragmented and covered at least 50% of the request were ranked for each HCN separately. The first 15 ranked contigs for each HCN were then compared among isoforms and when associated with multiple isoforms, assigned to the best ranked HCN. A phylogenetic tree was then generated as described above.

2.4. Statistical analysis

All statistical analyses were carried out using PAST3 (Hammer et al., 2001). For all treatments and isoforms, an initial $N = 6$ fish (i.e. organs) were used. As some samples were lost during processing, this resulted in varying $N = 4$–6 (more specifically indicated in Supp. Fig. 1). All data sets were tested for normal distribution (Shapiro–Wilk test) and homogeneity of variances (F-test). If one or both requirements were not met, data were log transformed where applicable and tested again. When criteria for parametric testing still were not met, non-parametric tests were performed instead. Consequently, criteria for the application of an Analysis of Variance (ANOVA) were neither met universally in the tissue distributions, nor across HCN isoforms and treatments. Alternatively, Kruskal-Wallis with pairwise Mann-Whitney *U* test was used in case of comparison of multiple means (Fig. 3) and Student's *t*-test or Mann-Whitney U test for comparison of single means (Figs. 4,5). To correct for multiple testing, α was adjusted sequentially as $\alpha_k = 1 - (1 - \alpha_{sign})\hat{}k$, with k as the number of multiple comparisons (k = 1–5 in Fig. 3 and k = 1–2 in Figs. 4,5). Subsequently, a Holm-Bonferroni correction was performed and significance considered accordingly at $P_k = \alpha i/(k\text{-}i)$. Graphs were generated using the software Inkscape, version 0.48 (https://inkscape.org/).

3. Results

3.1. Identification of CaHCN isoforms

Overall, in the *Cyprinus carpio* transcriptome, we identified two entries in the NCBI database for potential HCN1-like (GeneBank accession numbers **XM019082034.1**, **XM019116212.1**), seven entries annotated for HCN2-like (**XM019071468.1**, **XM019101656.1**, **XM019105399.1**, **XM019118763.1**, **XM019119676.1/XM019119677.1**, **XM019122180.1**), five entries annotated for HCN3-like (**XM019068612.1/XM019068613.1**, **XM019088348.1**, **XM019099869.1**, **XM019125329.1**) and three entries annotated for HCN4-like (**XM019116252.1**, **XM019123466.1/XM019123467.1**). Initially, representatives for each of the HCN isoforms were chosen based on the longest available / most comprehensive sequence, and most promising and consistent annotation in all NCBI-BLAST analyses (i.e. BLASTn, BLASTx; data not shown). Ultimately, successful and reliable amplification by qPCR in *Carassius auratus* was only achieved in a subgroup of these, namely **XM019082034.1** (HCN1-like), **XM019105399.1** (HCN2-like), **XM019068613.1** (HCN3-like) and **XM019116252.1** (HCN4-like). It needs to be noted that at the time of the sequence identification, primer design and qPCR analysis, an assembled *C. auratus* transcriptome and/or genome was not readily available in the NCBI database and no hits could be found for goldfish specifically. At the time of drafting this manuscript, an additional BLAST analysis was performed to identify the then available corresponding *C. auratus* contigs from its genome and they were identified as **XM026234417.1** (CaHCN1), **XM026198318.1** (CaHCN2), **XM026287017.1** (CaHCN3) and **XM026239097.1** (CaHCN4). These sequences were then consequently used to investigate tissue mRNA abundance patterns and their changes in response to feeding and/or HEA (Figs. 4,5). Unfortunately, **XM019068613.1** (*C. carpio*) and the corresponding *C. auratus* contig **XM026287017.1** were misleadingly annotated as HCN3-like in the NCBI database, but **XM026287017.1** turned out only later to resemble CaHCN4a (see below), and hence a representative for HCN3 is missing in the mRNA abundance analysis.

3.2. Phylogenetic analysis of HCN isoforms

Blasting the goldfish genome once it became available in NCBI revealed two isoforms each for CaHCN1 and CaHCN3 in *C. auratus*, whereas for CaHCN2 and CaHCN4 two paralogs with two isoforms each were obtained and used for the phylogenetic analyses (Figs. 1A, 2). For both the CaHCN tree and the multiple species tree, the evolutionary history was inferred by using the Maximum Likelihood method based on the Jones-Taylor-Thornton matrix-based model (Jones et al., 1992) (Figs. 1, 2). A discrete gamma distribution (+*G*; five categories) was used to model evolutionary rate differences among sites between all sequences included in the gene tree analysis (+*G* = 0.418 and 0.516 for CaHCN tree and multiple species tree, respectively). All positions with less than 95% site coverage were eliminated, resulting in a total of 802 and 396 positions in the CaHCN tree and the multiple species tree. Bootstrap analyses were performed with 500 replicates.

According to currently available information, the identified CaHCN paralogs have been labelled as CaHCN2a, CaHCN2b, CaHCN4a, and CaHNC4b, respectively (Figs. 1B, 2). The sequence initially annotated as CaHCN3 (**XM026287017.1**) in *C. auratus* seemed to rather represent CaHCN4a according to the present phylogenetic analysis (Fig. 2). While all mammalian and fish HCN1, HCN2, HCN3 and HCN4 formed distinct monophyletic groups and could be set apart from each other, HCN3 seem to be present in its own separate clade (Fig. 2). Our analysis supported HCN1 to be represented as one paralog, and HCN2, HCN3 and HCN4 to be represented as two paralogs (labelled as “a” and “b”, respectively). Overall, CaHCNs seemed to be most similar to *Danio rerio* representatives (HCN1, HCN2b, HCN4a, HCN4b) with the exception of CaHCN3 that rather clustered with *Salmo salar*. A sequence for HCN2a has yet to be identified in *D. rerio* and *Carassius auratus*.

3.3. Tissue distribution of HCN isoforms

Overall, mRNA abundance for all HCN isoforms was highest in brain and heart, between 5-fold (CaHCNsb/4b heart vs. gut) and 124-fold (CaHCN1 brain vs. gill).

Lowest overall expression was identified for CaHCN1 even though it was still present in all organs, albeit hardly detectable in the kidney (Fig. 3A, Supp. Fig. 1). The only exception was the brain, where CaHCN1 exhibited a similar mRNA expression level as CaHCN2b and CaHCN4a. CaHCN2b was the second most abundant isoform (after CaHCN4b) mostly in kidney and gut, but was also detected in gill and liver (Fig. 3B, Supp. Fig. 1). Still, CaHCN2b mRNA levels were between 5-fold (heart to gut) to 25-fold (brain to gill) higher in excitable vs. non-excitable organs. CaHCN1 and CaHCN2b also exhibited significantly lower mRNA abundance in brain compared to the heart. CaHCN4a was detected at moderate levels in brain and heart similar to CaHCN1 and CaHCN2b, low levels in gills and gut, and negligible or no detectable expression in kidney and liver, respectively (Fig. 3C, Supp. Fig. 1). Overall, CaHCN4b showed the highest mRNA abundance in all investigated organs compared to the other isoforms (Fig. 3D, Supp. Fig. 1), and particularly in gill and gut (8.9 and 4.6-fold higher than

A

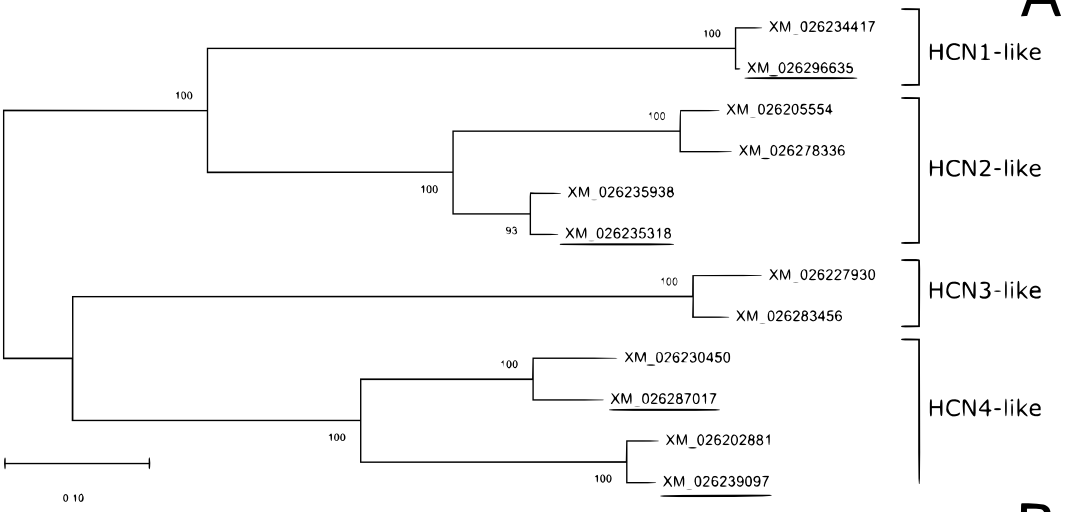

B

```
HCN1-XM_026196635      ------------------------------------------------------------ 0
HCN2-XM_026198318      -------------------------MDEAEDGDEDHKETRRGDILDSSYKMKRVTPGGGA 35
HCN4a-XM_026287017     MDRLHSSMRKRLYSLPQHIGQKAFIMGDAEDS---DKDTRRKS-----IRMKPLPSPTSE 52
HCN4b-XM_026239097     MDKVHSSMRKRLYSLPHQFGHKGAMTRDGEDS---DKDTRRKS-----VKMKHLPSPSST 52

HCN1-XM_026196635      ------------------------------------------------------MEDKSN 6
HCN2-XM_026198318      AASRISNNKDFASVSCGRSTESTALLCHGDAARDKSGVDGEDGSGMRCVINGDCRRDESL 95
HCN4a-XM_026287017     --------------------GETR----S---GESVIMETDIGRPVKTSSNGDCRRFRGS 85
HCN4b-XM_026239097     --------------------GSSK----GVSEAKSGDAETDVGKPFRTNVNGDCRRFRGS 88
                                                                          . ..

HCN1-XM_026196635      SFSSNKEEKADGNNVF--------------------------QRQDSILK-----NSMGS 35
HCN2-XM_026198318      SSTLSKQEKQTGGGFPASACHSSTSSMDGSVTPAPTAAAPPAEKKDSRVSFSSAPPTQGS 155
HCN4a-XM_026287017     LSSITSRHVHD-SDVAEERRLIT----EGEATP--SEESPPGAAGGGGEDEDA--AGASQ 136
HCN4b-XM_026239097     LSSITSRHAPD-ADLAEQRCLIA----DAS--P--EDDGPLEQPGPGESLGAQ--GGRGE 137
                        : ....     ..                                .           ..

HCN1-XM_026196635      -QNMKDHGNSVGAKGDREEAMVGFDDMDAASRQSGFMQRQFGAMMQPGVNKFSLRMFGSQ 94
HCN2-XM_026198318      SSNQPQPDSSVGFPKS-EDGQITADD-AEARDNQTYMQRQFSSMLQPGVNKFSLRMFGSQ 213
HCN4a-XM_026287017     QQQPGVPDQQAGFIKLEGIEQIL--PDDERYYQEGFMHRQFGAMLQPGVNKFSLRMFGSE 194
HCN4b-XM_026239097     GAQQAPSEEQSSFVKLEGIDQIM--PDDERLYQAGFMHRQFGAMLQPGVNKFSLRMFGSE 195
                         :     .. .         :          :  :*:***.:*:***************:

HCN1-XM_026196635      KAVEKEQERVQTAGYWIIHPYSDFRFYWDLIMLIMMMGNLIIIPVGITFFSEQTTTSWLI 154
HCN2-XM_026198318      KAVEKEQERVKSAGNWIIHPYSDFRFYWDFTMLMFMVGNLIIIPVGITFFKEETTTPWII 273
HCN4a-XM_026287017     KAVEREQERVKSAGYWIIHPYSDFRFYWDLTMLLLMVGNLIIIPVGITFFKDEHTPPWIV 254
HCN4b-XM_026239097     KAVEREQERVKSAGFWIIHPYSDFRFYWDLIMLLLMVGNLIIIPVGITFFKDEHTPAWIV 255
                       ****:*****::** ***************: **::*:*************.:: *  *::
                      [155-274 / 274-393 / 256-375 / 255-374 excluded from view]

HCN1-XM_026196635      IFNLIGMMLLLCHWDGCLQFLVPLLQDFPPDCWVSLNGMVNDSWGKQYSYALFKAMSHML 334
HCN2-XM_026198318      IINLIGMMLLLCHWDGCLQFLVPMLQDFPSDCWVSLNKMVNDSWSELYSFALFKAMSHML 453
HCN4a-XM_026287017     IVNLIGMMLLLCHWDGCLQFLVPMLQDFPQDCWVSKNKMVNDTWGQQYSYALFKAMSHML 434
HCN4b-XM_026239097     IVNLIGMMLLLCHWDGCLQFLVPMLQDFPSDCWVAKNNMVNDTWGQQYSYALFKAMSHML 435
                       *.**********************:***** ****: * ****:*.: **:**********
                      [335-574 / 454-693 / 435-675 / 435-674 excluded from view]

HCN1-XM_026196635      NSLLLQKFQKDLNAGVFNTQENELLKQIIRQDREMVMMVDRKQS--VTGMNS-TPMSGNS 631
HCN2-XM_026198318      NSILMHKVQHDLNSGVFNNRENEMIQEIVKYDREMVKLVKQGDMQRPRAMSM-TPSTQGN 752
HCN4a-XM_026287017     NSILQHKVQHDLNSGVLNYQESEIIQQIVQHDRDMAHCANLMQSPSPPA----PPSPTPV 730
HCN4b-XM_026239097     NSVLQHKVQRDLNSGVLNYQENEIIQQIVQHDRDMAHCAHLMQTPPPASHPAVTPSHTPV 735
                       **:* :*.*:***:**:* :*.*::::*:: **:*.  ..  :     .     *

HCN1-XM_026196635      IINSPAQPPFTTAIA-------ILGNNQLQQQAAPLSYSTSATITPSGRVPPSQGVTFSA 684
HCN2-XM_026198318      IFTPSSQPSTSSAIA-------SLQQ------AVAMSFCPQ------MGNPLVGAGAVQS 793
HCN4a-XM_026287017     IWAPLIQAPLQAAAATTSVAIALTHHPHLP----ASLFRPPVSILGS---------RNEP 777
HCN4b-XM_026239097     IWAPLIQAPLQAAAATTSVAIALTRHPHLP----HTLFRPPVPLLGS---------LKDQ 782
                       *     *    :* *          :          :                    .
```

(caption on next page)

Fig. 1. Sequence analysis of hyperpolarization-activated cyclic nucleotide gated potassium channels (HCN) in *Carassius auratus* as investigated in this study. (A) Molecular phylogenetic analysis of all identified HCN proteins in the *C. auratus* genome as available in the NCBI database by the Maximum Likelihood method. The evolutionary history was inferred by using the JTT matrix-based model (Jones et al., 1992). The tree with the highest log likelihood (−8262.74) is shown. Numbers at each branch indicate the percentage of trees in which the associated taxa clustered together. The tree is drawn to scale, with branch lengths measured in the number of substitutions per site. Evolutionary analyses were conducted in MEGA X (Kumar et al., 2018). Underlined contigs indicate the isoforms that have been investigated in the present study by quantitative real-time PCR analysis. (B) Alignment of all CaHCN protein sequences using the ClustalOmega-tool as provided by the EMBL database (https://www.ebi.ac.uk/Tools/msa/clustalo/). Bold underlined fragments indicate the amplified fragments for qPCR. "." indicate conservation of weak groups, ": " indicate conservation of strong groups and "*" indicate sequence identity. Part of the alignment (not containing any fragments of interest) has been truncated as indicated in the graph to minimize its size.

CaHCN2b in gill and gut, respectively). It also exhibited the highest level of variation.

3.4. Changes in mRNA abundance of HCN isoforms in response to a feeding or HEA

3.4.1. Feeding

In response to feeding, CaHCN1 was the only one among all isoforms that was significantly up-regulated, which was the case in the kidney by 2.5-fold (Fig. 4A). Additionally, a down-regulation in response to feeding was observed for CaHCN2b in the gut (78%, Fig. 4B). Non-significant tendencies (after Holm-Bonferroni correction) were observed for CaHCN4a to be down-regulated in the gill (57.5%) and heart (63%, Fig. 4C) and CaHCN4b in the kidney (73%, Fig. 4D). The most pronounced changes in mRNA abundance in response to feeding were observed for CaHCN4a which exhibited a complete shut-down in the gut (Fig. 4C).

3.4.2. High environmental ammonia (HEA)

The mean measured in-tank values during HEA exposure were pH = 6.87 ± 0.04, 2317 ± 161 μmol L^{-1} total ammonia. Goldfish exposed to HEA were able to excrete ammonia against this high outside concentration at a rate of 7.2 ± 1.4 μmol h^{-1} g^{-1} (mean ± SE, $N = 6$). Exposure to HEA affected mRNA abundance in a different suite of CaHCN isoforms than feeding and resulted in overall more numerous and higher magnitude changes (Fig. 4). None of the isoforms were significantly affected by both treatments. CaHCN4a was the only isoform, however, that exhibited the tendency for down-regulation in both the gill and the heart upon both feeding (57% and 63%) and significantly upon HEA exposure (100% and 82%, respectively).

In response to HEA, CaHCN1 was significantly up-regulated in gut and brain (3.1- and 1.7-fold, respectively; Fig. 4A). CaHCN2b showed a pronounced down-regulation in liver and heart (82% and 52%), albeit not significant in the liver. It also exhibited a tendency for up-regulation in brain (1.3-fold; Fig. 4B). CaHCN4a exhibited marked changes in the kidney, where initially it was not expressed at all but after exposure to HEA exhibited one of the overall highest expression levels. Contrastingly in the gill, expression of CaHCN4a was completely shut-down in response to HEA. Additionally, CaHCN4a was significantly up-regulated in the brain (1.3-fold) and down-regulated in the heart (82%, Fig. 4C). No changes in mRNA abundance of CaHCN4b were observed in response to HEA (Fig. 4D).

Notably, most isoforms exhibited a much higher variance in response to HEA in the kidney (CaHCN1, CaHCN4a, CaHCN4b) compared to the other tissues, as well as in comparison to the responses to feeding.

3.5. Changes in mRNA abundance of Rhesus glycoproteins

Rhesus-protein isoform bg (Rhbg) was the only Rhesus glycoprotein that could be detected in the brain where it was significantly up-regulated in response to both feeding and exposure to HEA (2- and 3-fold, respectively; Fig. 5A). Rhcg1 on the other hand exhibited a 2.5-fold up-regulation in response to HEA exposure in the kidney, as well as a non-significant (50%) down-regulation in response to feeding in this tissue (Fig. 5B). While not detected in fasted animals, Rhcg2 mRNA expression switched on in response to both feeding and HEA acclimation, and more markedly so in the latter case (Fig. 5C). However, this response was not observed in all samples and in some animals the mRNA expression of this gene remained undetectable. No significant changes of any Rhesus glycoprotein were observed in the gill.

4. Discussion

4.1. Phylogeny of CaHCN

In the present study, we were able to identify six *C. auratus* HCN paralogs (CaHCN1, CaHCN2a, CaHCN2b, CaHCN3, CaHCN4a, CaHCN4b), all of which were present as two distinguishable isoforms. The phylogenetic analysis of the identified goldfish paralogs supports HCN3 to be the most ancient as also suggested by Jackson and colleagues (Jackson et al., 2007), and hence it might have served as the "template" for the duplication event. Interestingly, and in contrast to hagfishes (Wilson et al., 2013) or other teleosts (Hassinen et al., 2017; Jackson et al., 2007), we could only identify a single CaHCN3 paralog in goldfish represented by two different isoforms, while our phylogenetic analysis supports the presence of two HCN3 paralogs in other fish, as evident here for *Salmo salar*. It remains possible that the current analysis simply failed to identify a second paralog CaHCN3b. Furthermore, as in all other fishes, CaHCN1 seems to be present as only one paralog. Being the most recent gene in the HCN family, HCN1 might not have undergone a duplication event itself as proposed by Jackson and colleagues (Jackson et al., 2007) and might only have appeared after the divergence of HCN2.

4.2. Potential role of CaHCNs in regulating acid-base and ammonia-disturbances

The presence of the relatively large number of CaHCN paralogs and isoforms in *C. auratus* and other teleosts and their overall high level of conservation both attest to the importance of this transporter family. As expected, all goldfish CaHCNs exhibited their highest mRNA abundance in brain and heart. Interestingly, the fact that CaHCN4b is the predominant isoform in all tissues (and specifically in heart and brain) resembles the situation in mammals (Biel et al., 2009) and not hagfish, as in the latter HCN3a seems to dominate (Wilson et al., 2013). It should be noted that differences of one specific HCN isoform across all organs might partly be due to the presence of enclosed excitatory tissues, as organs were harvested as a whole. When looking at all/multiple HCN isoforms in one particular organ, however, it becomes clear that there likely is also a non-excitatory tissue distribution; for example, while CaHCN2b and CaHCN4a have a very similar expression in excitable tissues alone (i.e. brain and heart), CaHNC2b clearly dominates CaHCN4a expression in all other organs. The apparent tissue specificity of CaHCNs and presence in non-excitable tissues might hence indicate a physiological function that has received little investigation to date (in addition to their well-known roles in cardiac pacemaker and nerve conduction). For example, CaHCN2b showed a relatively high mRNA abundance in gut and kidney. Carrisoza-Gaytán and colleagues (Carrisoza-Gaytán et al., 2011) demonstrated that HCN2 in rat was able to promote NH_4^+ transport and to participate in renal acid-base regulation specifically in the non-excitable, acid-secreting intercalated cells of the connecting tubule and collecting ducts. Furthermore, HCN1

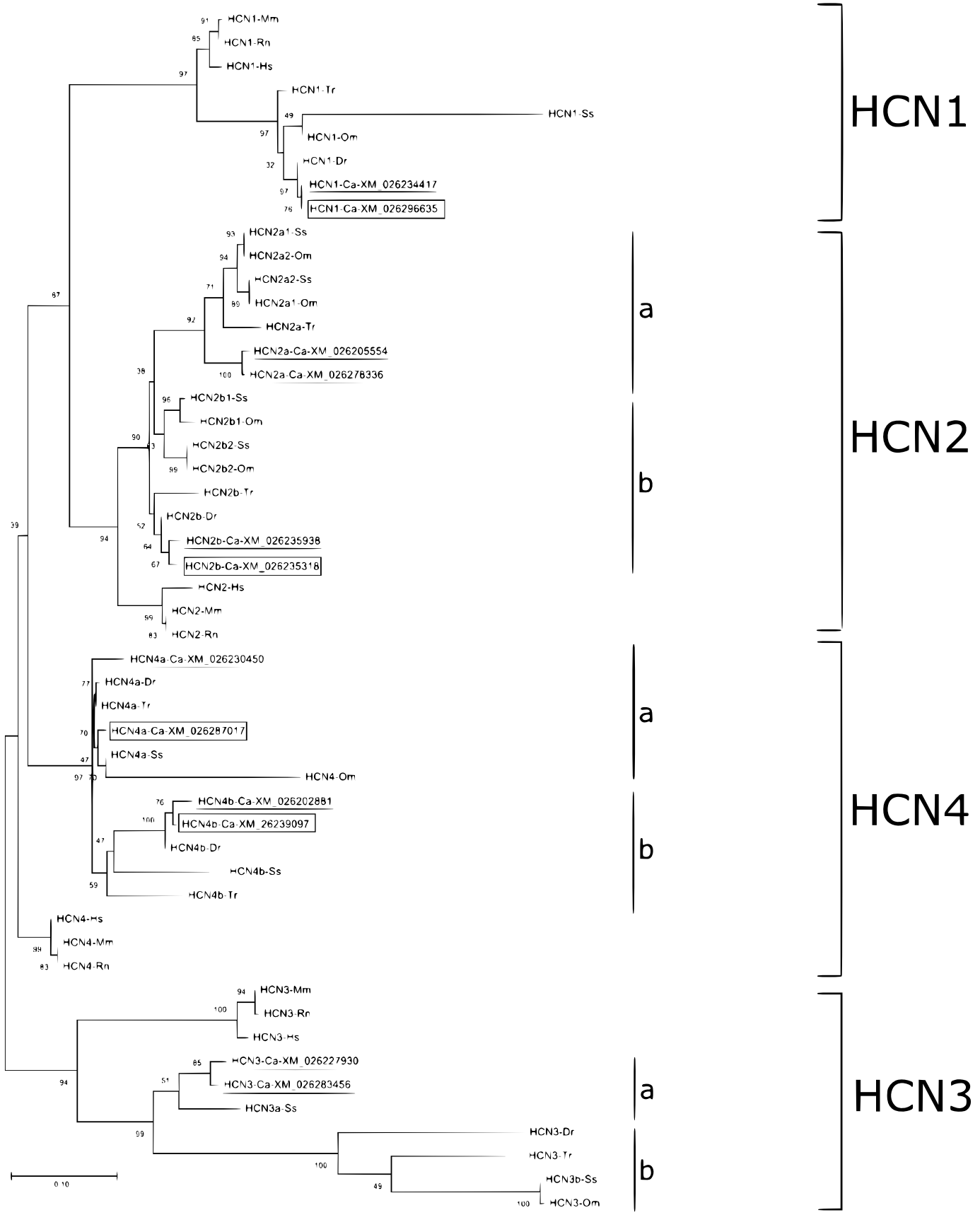

(caption on next page)

Fig. 2. Molecular phylogenetic analysis of HCN proteins by the Maximum Likelihood method. The evolutionary history was inferred by using the JTT matrix-based model (Jones et al., 1992). The tree with the highest log likelihood (−4958.19) is shown. The percentage of trees in which the associated taxa clustered together is shown next to the branches. The tree is drawn to scale, with branch lengths measured in the number of substitutions per site. Evolutionary analyses were conducted in MEGA X (Kumar et al., 2018). Ca, *Carassius auratus*; Dr, *Danio rerio*; Hs, *Homo sapiens*; Mm, *Mus musculus*; Om, *Oncorhynchcus mykiss*; Rn, *Rattus norvegicus*; Ss, *Salmo salar*; Tr, *Takifugu rubripes*. Proteins investigated in this study are indicated by boxes, while the rest of the identified isoforms in the *C. auratus* genome are underlined. Gene accession numbers are referred to in Supplementary Table 1.

and HCN3 seem to play a role in rat renal acid-base and K^+ homeostasis in response to feeding (López-González et al., 2016). A HCN was also identified to participate in branchial acid-base and ammonia regulation in the green crab, *Carcinus maenas* (Fehsenfeld and Weihrauch, 2016).

Most relevant might be the finding that HCN-mediated currents are sensitive to pH (i.e. intra- as well as extracellular $[H^+]$). That is, an increase in intracellular $[H^+]$ shifted channel activation of murine HCN2 expressed in HEK293 cell cultures to require more hyperpolarization of the membrane (Zong et al., 2001), while an increase in extracellular $[H^+]$ activated HCN1 and HCN4 channels in rat taste cells (Stevens et al., 2001). Furthermore, the ionic composition of body fluids and particularly extracellular $[K^+]$ (and therefore potentially also $[NH_4^+]$ due to its similar charge and size (Towle and Holleland, 1987)) determines HCN transport properties (Frace et al., 1992). With regard to the experimental treatments used in the present study, both extracellular $[H^+]$ (Wood et al., 2010) and plasma ammonia levels (Liew et al., 2013; Sinha et al., 2012b) increase in response to feeding in agastric fish like the goldfish. Furthermore, the activity of Na^+/K^+-ATPase (NKA), which generates a negative potential across basolateral cellular membranes (Skou, 1960) and establishes a K^+ concentration gradient to facilitate its diffusion, was observed to increase with feeding in gills and intestine of goldfish (Turner and Bucking, 2017). An increase in NKA activity would lead to hyperpolarization of the basolateral membrane and hence activate HCNs. Exposure to HEA also led to elevated extracellular [ammonia], as well as an activation of NKA (Sinha et al., 2012a).

We postulate that HCNs can participate in acid-base and ammonia homeostasis in two different ways: (i) the restoration of membrane potential in excretory epithelial cells i.e. complementing changes in activity of the basolateral NKA, and/or (ii) through direct NH_4^+ transport. Consequently, feeding might lead to H^+-mediated basolateral HCN activation (i.e. HCN1, HCN4). In this scenario, more extracellular NH_4^+ would be able to enter the cell to then be secreted apically, likely with the help of Rhesus proteins and especially apical

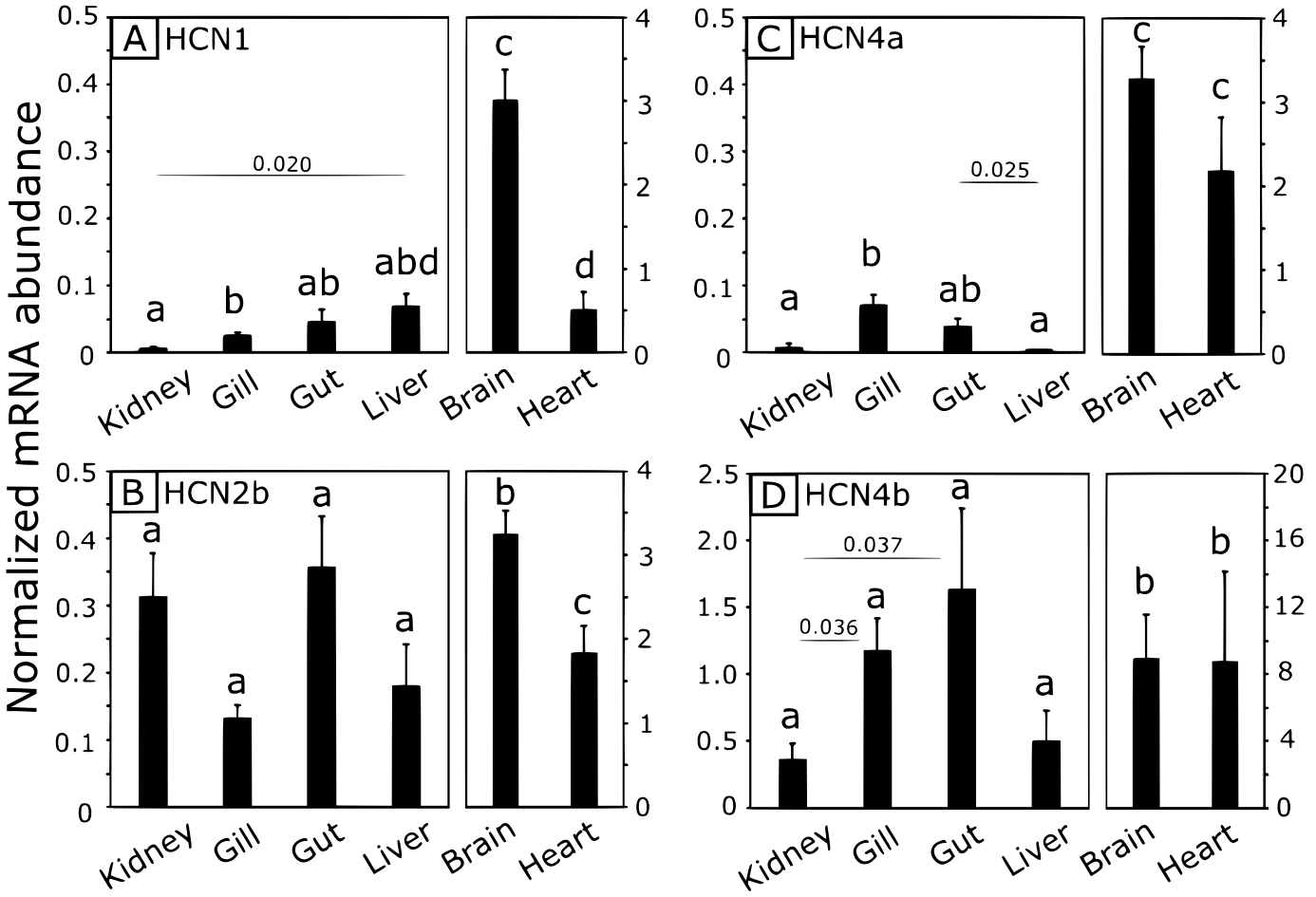

Fig. 3. Tissue mRNA abundance of the investigated CaHCN isoforms. (A) CaHCN1, (B) CaHCN2b, (C) CaHCN4a, and (D) CaHCN4b. mRNA expression has been normalized to BA*Ef1α. Data are expressed as fold-change (mean + SE, N = 4–6, see also Supp. Fig. 1). Please note the different scale for brain and heart as indicated at the y-axis on the right side. Lower case letters indicate significant differences (Kruskal-Wallis with Mann-Whitney U test and Holm-Bonferroni correction). Sequential P_k values were determined based on sequentially adjusted α values according to $\alpha_k = 1 - (1 - \alpha_{sign})^k$, with k as the number of multiple comparisons and accounted to P_1 = 0.01, P_2 = 0.0125, P_3 = 0.017, P_4 = 0.025, P_5 = 0.05 (see Material and Methods for details). Numbers indicate all original P values < .05 that are not considered significant after Holm-Bonferroni correction.

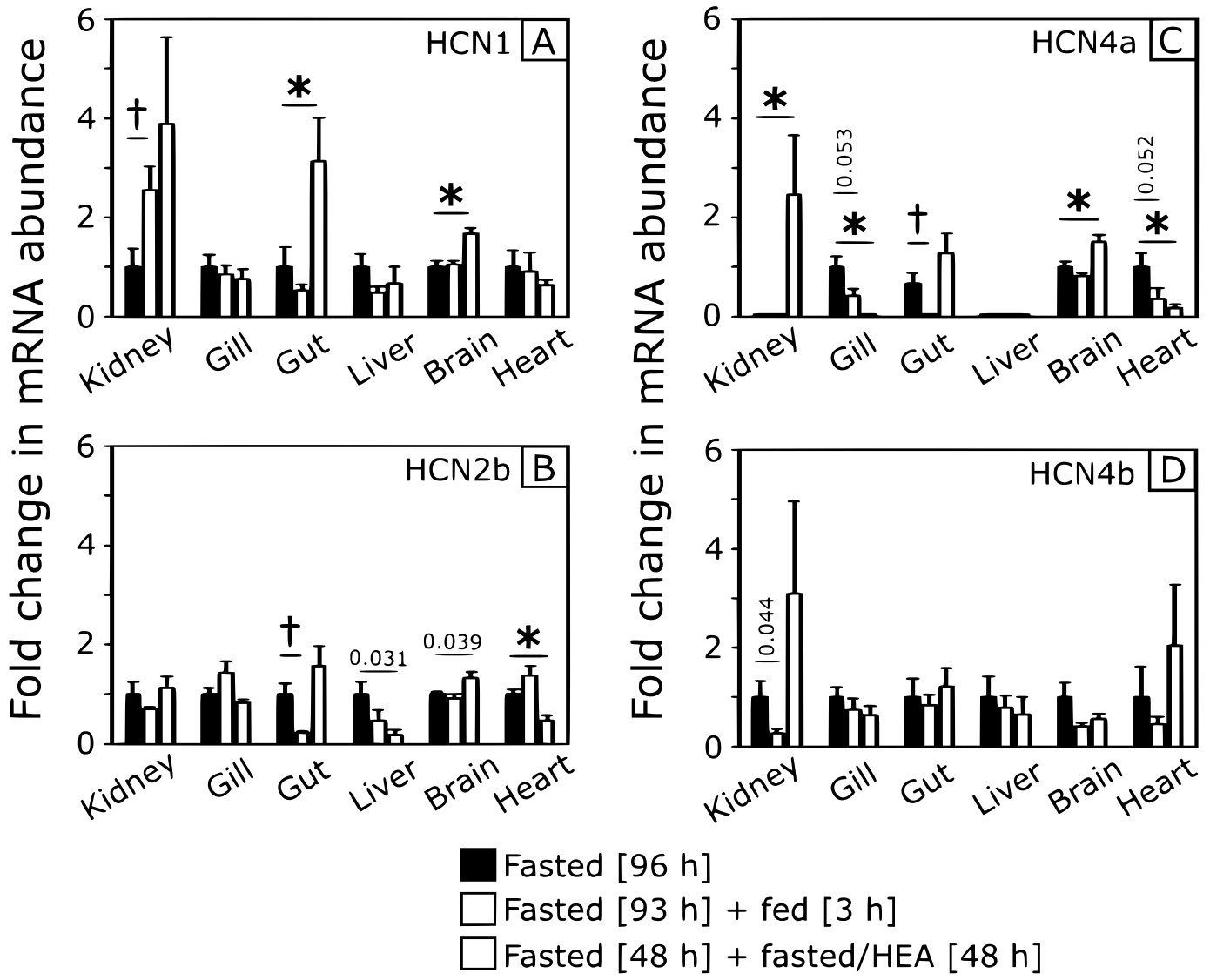

Fig. 4. A comparison of mRNA abundance of the investigated CaHCN isoforms across organs in response to feeding and high environmental ammonia. (A) CaHCN1, (B) CaHCN2, (C) CaHCN4a, (D) CaHCN4b. mRNA expression has been normalized to BA*Ef1α. Significant differences are indicated by a dagger for significant differences between fasted and fed conditions and asterisks for significant difference between fasted and fasted/HEA conditions (Student's *t*-test or Mann-Whitney U test with Holm-Bonferroni correction). Sequential P_k values were determined based on sequentially adjusted α values according to $\alpha_k = 1 - (1 - \alpha_{sign})^k$, with k as the number of multiple comparisons and accounted to $P_1 = 0.025$ and $P_2 = 0.05$ (see Material and Methods for details). Numbers indicate values for $0.05 > P > .025$ that are not considered significant after Holm-Bonferroni correction and are vertically aligned for fasted vs. fed and horizontally aligned for fasted vs. fasted/HEA. comparisons. Black bars are fasted animals; white bars are fed animals; grey bars are fasted/HEA-exposed animals. Values are expressed as fold-change (mean + SE, with $N = 4–6$).

Rhcg2 (Fehsenfeld et al., 2019; Fehsenfeld and Wood, 2018). An increase in NKA activity due to feeding and/or HEA exposure would lead to hyperpolarization of the basolateral membrane and subsequently also activate basolateral HCN(s). In this case, the HCN(s) would function to either restore membrane potential via increased basolateral entry of K^+, or again to help clear an extracellular NH_4^+-load as described above.

4.3. Differential changes in mRNA abundance of specific HCN isoforms and Rhesus glycoproteins

Acid-base challenges in goldfish provoked by either feeding (internal acid- and ammonia-load, Fehsenfeld and Wood, 2018; Wood et al., 2010) and/or exposure to high environmental ammonia (resulting in an internal ammonia load, Sinha et al., 2012b) resulted in differential responses of different HCN isoforms and Rhesus glycoproteins at the mRNA level. While generally the HEA treatment significantly impacted mRNA abundance in a higher number of cases (7 significant differences for HCNs and 3 for Rhesus glycoproteins in response to HEA vs. 3 significant differences for HCNs and 1 for Rhesus glycoproteins in response to feeding), CaHCN4a in the gill and heart as well as Rhbg in the brain appeared to be the only transcripts affected by both feeding and HEA.

4.3.1. Kidney vs. gill

CaHCN1 was the only HCN isoform for which mRNA abundance was up-regulated in the kidney in fed goldfish. Together with the observed up-regulation of apical Rhcg2 (Rhcg1b) and potential down-regulation of (basolateral) Rhcg1 (Rhcg1a) (present study, Fehsenfeld et al., 2019; Fehsenfeld and Wood, 2018), this HCN isoform - when situated basolaterally as in hair cells in the ear of the mouse (Horwitz et al., 2010) - might be involved in renal excretion of the feeding-

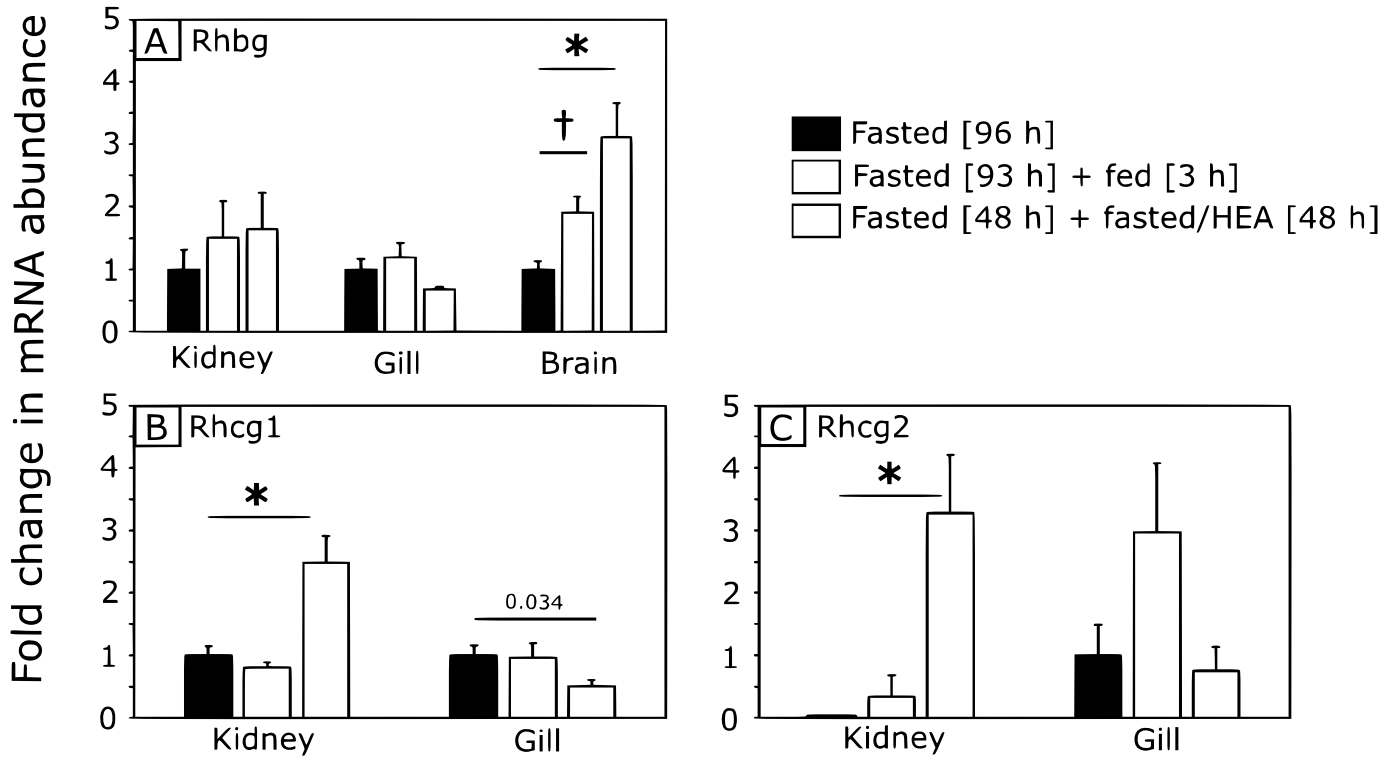

Fig. 5. A comparison of mRNA abundance of Rhesus glycoproteins across organs in response to feeding and high environmental ammonia. (A) Rhesus-protein Rhbg (B) Rhcg1, (C) Rhcg2. mRNA expression has been normalized to BA*Ef1α. Significant differences are indicated by daggers for significant differences between fasted and fed conditions and asterisks for significant difference between fasted and fasted/HEA conditions (Student's t-test or Mann-Whitney U test with Holm-Bonferroni correction). Sequential *P* values were determined as $P_1 = 0.025$ and $P_2 = 0.05$ (see Material and Methods for details). Numbers indicate values for $0.05 > P > .025$ that are not considered significant after Holm-Bonferroni correction and are horizontally aligned for fasted vs. fasted/HEA. comparisons. Black bars are fasted animals; white bars are fed animals; grey bars are fasted/HEA-exposed animals. Values are expressed as fold change (mean + SE, with $N = 4–6$).

induced ammonia-load and/or acid-load in synergy with Rhcg2. A potential activation of HCN1 in response to increased extracellular H^+ due to the feeding-induced acidic tide (Wood, 2019; Wood et al., 2010) is in accord with observations in rat and mouse when vallate papilla were stimulated by a “sour”/acidic (i.e. H^+-mediated) stimuli (Stevens et al., 2001).

Neither feeding nor HEA exposure evoked any response of CaHCN2b in the kidney. This is in contrast to what could have been expected according to observations in the mammalian kidney as mentioned above (i.e. down-regulation of HCN2 in rat kidney in response to metabolic acidosis (Carrisoza-Gaytán et al., 2011)). Unfortunately, no mRNA expression data for CaHCN2a were obtained in the present study. It would be of interest to see if this isoform undergoes more pronounced changes in response to feeding and/or HEA exposure.

CaHCN4a seems a particularly interesting candidate for involvement in ammonia handling in the kidney as it was initially not expressed but then switched on in response to HEA. Simultaneously, mRNA abundance of both renal Rhcg1 (Rhcg1a) and Rhcg2 (Rhcg1b) were increased in response to HEA so that all three channels could work together to maintain kidney function by increasing ammonia excretion while at the same time restoring membrane potential. CaHCN4a was the only HCN isoform to be affected in the gill and responded to both treatments, feeding and HEA. In contrast to the kidney, however, CaHCN4a was switched off in the gill in response to HEA. At the same time, we observed no changes in branchial Rhcg1 and Rhcg2 mRNA abundance after 48 h of HEA exposure, which is in accord with the study of Sinha and colleagues (Sinha et al., 2013) that found these genes to be up-regulated, but only after 84 h. This indicates a role for the gill and specifically CaHCN4a in counteracting the HEA-induced ammonia disturbance potentially only later on and the renal response to proceed as has been suggested by Fehsenfeld and Wood (Fehsenfeld and Wood, 2018). The observed down-regulation of gill CaHCN4a expression might hence only serve as an early-onset protective mechanism to prevent NH_4^+ uptake from the plasma if indeed situated basolaterally as observed for HCN4 in rat and mouse vallate papilla (Stevens et al., 2001), or from the HEA environment if localized in the apical membrane.

4.3.2. Gut and liver

The presence of HCNs in the gut might be related to the generation of pulses for peristaltic movements (Shahi et al., 2014). Alternately or additionally, they may play a role in N-homeostasis. Feeding in goldfish would increase Na^+/K^+-ATPase activity in intestine (Turner and Bucking, 2017) and decrease plasma pH (Wood et al., 2010). Both factors would lead to an activation of basolateral HCN channels, potentially resulting in ammonia transport out of the intestinal blood plasma and efflux to the intestinal lumen - by substitution of NH_4^+ for K^+ and the inward direction (plasma to cytoplasm) of the HCN-generated current (Biel et al., 2009). However, as a herbivore (Sarbahi, 1951), the goldfish is probably N-limited and must attempt to absorb nitrogen from their diet, as proposed for the carnivorous trout (Rubino et al., 2019). The observed down-regulation in response to feeding of the two HCN paralogs CaHCN2b and CaHCN4a that are likely basolaterally localized (Carrisoza-Gaytán et al., 2011; Stevens et al., 2001) might hence help to conserve ammonia. In contrast, during HEA, the up-regulation of a basolateral CaHCN1 (Horwitz et al., 2010) might be necessary to meet increases in NKA activity and restore membrane potential. Clearly there are competing influences here that deserve future study.

In the liver, our data do not indicate a substantial role for HCN-mediated responses to feeding or HEA.

4.3.3. Brain

In the rainbow trout, HEA exposure led to an increase of ventilation that was correlated with increased brain ammonia levels and increased Rhbg mRNA expression in the brain (Zhang et al., 2013). The authors proposed that the elevated Rhbg served to accelerate ammonia flux from the central nervous system, to be excreted by the gills. In support of this hypothesis, the present goldfish also up-regulated mRNA for Rhbg 3-fold in the brain upon exposure to HEA while maintaining overall ammonia excretion, and also increased Rhbg expression 2-fold in response to feeding. Notably, CaHCN1 mRNA expression was highest in brain (6-fold compared to heart, 43-fold compared to liver) at a similar level compared to CaHCN4a, and both paralogs were up-regulated by a similar degree in the brain in response to HEA. This might indicate a synergistic role for Rhbg and CaHCN1/CaHCN4a to secure cell function. Potentially elevated entry of NH_4^+ into the cell via CaHCN1/CaHCN4a might be countered by NH_4^+ exit through Rhbg in order to maintain the cellular membrane potential.

4.3.4. Heart

In contrast to the brain where all affected HCN isoforms (CaHCN1, CaHCN4a and potentially CaHCN2b) were up-regulated in response to HEA, all affected HCN isoforms in the heart were down-regulated (CaHCN2b, CaHCN4a in response to HEA, and CaHCN4a potentially also to feeding). This suggests a direct role for a combination of different HCN channels in the orchestration and protection of the heartbeat from elevated extracellular plasma ammonia levels and $[H^+]$, as well as resulting increase in NKA activity, that would activate HCNs. As mentioned earlier this appears similar to the mammalian function of HCNs in cardiac function with a predominance of HCN4, in contrast to hagfish where HCN3a is the predominant cardiac isoform (Wilson et al., 2013). A protective mechanism for the heartbeat with the help of HCNs has been suggested before for ammonia-sensitive (rainbow trout *Oncorhynchus mykiss*) and ammonia-tolerant fish (oriental weatherloach *Misgurnus anguillicaudatus*) (Tsui et al., 2004).

4.4. Constraints and future directions

The present study focused on the molecular identification and characterization of HCN isoforms at the mRNA level, and less on anchoring our approach in physiological endpoints. We recognize that not all changes in mRNA abundance may translate into changes in protein expression and/or activity. While consequently this approach may have only limited implications for actual HCN function, the provided information lays the important groundwork for more detailed physiological investigations. In our recent study on ion transporters in the goldfish kidney (Fehsenfeld and Wood, 2018), mRNA abundance did indeed correlate very well with protein expression. Furthermore, with HCNs being so highly conserved on the protein level, a mRNA-centered approach might actually be the only approach for characterizing the roles of the different isoforms.

While we chose our treatments (i.e. feeding and HEA) based on the available literature to elucidate challenges for acid-base and ammonia homeostasis, every stressor has to be considered to result in a complex mixture of all kinds of physiological responses. Consequently, the changes in mRNA abundance that we observed might additionally be due to changes including general ion regulation / exchange or changes in metabolic rate, or effects associated with handling. It would hence be interesting for future studies to apply other acid-base / ammonia challenges and compare the responses – for example, low environmental pH or high environmental PCO_2.

It should also be noted that because we worked with isolated organs, rather than tissues free of nerves and muscle, a background level of HCN mRNA expression could be expected based on excitable cells contained within the organ. However, as mentioned above, renal HCN2 has been shown to be localized clearly also in non-excitable tissues within an organ (i.e. the basolateral membranes of acid-secreting intercalated and principal cells in the cortex and medulla in the rat kidney (Carrisoza-Gaytán et al., 2011)) so this is also likely to be the case in goldfish. Future research should entail further cell-specific localization of the CaHCN isoforms to clarify their specific expression patterns in the goldfish.

Despite its potential limitations, the current study provides novel information about the important family of HCN channels and is the first to look at them in a non-excitatory context in a teleost fish.

5. Conclusion

Despite the known ability of HCN channels to transport NH_4^+, and their well-documented pH-sensitivity, their potential contributions to more general physiological functions (other than to cardiac pacemaking and nerve conduction) have received relatively little investigation. The present study shows that mRNA abundance of specific HCN paralogs significantly changed in goldfish in response to an either internal (feeding) or external (high environmental ammonia) acid-base and/or ammonia disturbances in non-excitable tissues such as gills and kidney, the two key-organs for acid-base and ammonia regulation in teleosts. In addition, potential non-excitatory roles for HCN channels in the gut and brain are indicated, or alternatively, gut peristaltic and signal transduction might be part of restoring acid-base and ammonia homeostasis. Furthermore, changes in expression of Rhesus glycoproteins paralleled some of the observed changes in HCN expression. In a gene family exhibiting a level of amino acid conservation as high as seen in the HCN family, the generation of isoform-specific antibodies will be challenging. Our mRNA-based study hence provides promising groundwork for more detailed functional studies. Clearly, further research is needed to establish the exact mode of action and involvement for HCN channels in functions other than cardiac rhythmicity and neural excitability.

Author contributions

SF and CMW conceived the study. All experiments and analyses were performed by SF. SF wrote the original draft, while CMW reviewed and edited the manuscript.

Funding

This work was supported by a Discovery Grant from the Natural Sciences and Engineering Research Council of Canada to CMW (NSERC PIN-2017-03843).

Declaration of Competing Interest

The authors declare no competing or financial interests.

Acknowledgements

The authors thank Rachel Sutcliff (UBC) for sharing fish HCN sequences and contigs.

Appendix A. Supplementary data

Supplementary data to this article can be found online at https://doi.org/10.1016/j.cbpb.2020.110469.

References

Andersen, C.L., Jensen, J.L., Ørntoft, T.F., 2004. Normalization of real-time quantitative reverse transcription-PCR data: a model-based variance estimation approach to identify genes suited for normalization, applied to bladder and colon cancer data sets. Cancer Res. 64, 5245–5250. https://doi.org/10.1158/0008-5472.CAN-04-0496.

Biel, M., Wahl-Schott, C., Michalakis, S., Zong, X., 2009. Hyperpolarization-activated cation channels: from genes to function. Physiol. Rev. 89, 847–885. https://doi.org/10.1152/physrev.00029.2008.

Carrisoza-Gaytán, R., Rangel, C., Salvador, C., Saldaña-Meyer, R., Escalona, C., Satlin, L.M., Liu, W., Zavilowitz, B., Trujillo, J., Bobadilla, N.A., Escobar, L.I., 2011. The hyperpolarization-activated cyclic nucleotide-gated HCN2 channel transports ammonium in the distal nephron. Kidney Int. 80, 832–840. https://doi.org/10.1038/ki.2011.230.

Fehsenfeld, S., Weihrauch, D., 2016. The role of an ancestral hyperpolarization-activated cyclic nucleotide-gated K^+ channel in branchial acid-base regulation in the green crab, *Carcinus maenas*. J. Exp. Biol. 219, 887–896. https://doi.org/10.1242/jeb.134502.

Fehsenfeld, S., Wood, C.M., 2018. Section-specific expression of acid-base and ammonia transporters in the kidney tubules of the goldfish *Carassius auratus* and their responses to feeding. Am. J. Physiol. Ren. Physiol. 315, F1565–F1582. https://doi.org/10.1152/ajprenal.00510.2017.

Fehsenfeld, S., Kolosov, D., Wood, C.M., O'Donnell, M.J., 2019. Section-specific H^+ flux in renal tubules of fasted and fed goldfish. J. Exp. Biol. 222, 1–9. https://doi.org/10.1242/jeb.200964.

Frace, A.M., Maruoka, F., Noma, A., 1992. External K^+ increases Na^+ conductance of the hyperpolarization-activated current in rabbit cardiac pacemaker cells. Pflugers Arch. 421, 94–96.

Hammer, Ø., Harper, D.A.T., Ryan, P.D., 2001. PAST: Paleontological statistics software package for education and data analysis. Palaeontol. Electron. 4, 1–9. https://doi.org/10.1016/j.bcp.2008.05.025.

Hassinen, M., Haverinen, J., Vornanen, M., 2017. Small functional I_f current in sinoatrial pacemaker cells of the brown trout (*Salmo trutta fario*) heart despite strong expression of HCN channel transcripts. Am. J. Phys. Regul. Integr. Comp. Phys. 313, R711–R722. https://doi.org/10.1152/ajpregu.00227.2017.

Horwitz, G.C., Lelli, A., Géléoc, G.S.G., Holt, J.R., 2010. HCN channels are not required for mechanotransduction in sensory hair cells of the mouse inner ear. PLoS One 5https://doi.org/10.1371/journal.pone.0008627. (e8627–e8627).

Jackson, H.A., Marshall, C.R., Accili, E.A., 2007. Evolution and structural diversification of hyperpolarization-activated cyclic nucleotide-gated channel genes. Physiol. Genomics 29, 231–245. https://doi.org/10.1152/physiolgenomics.00142.2006.

Jones, D.T., Taylor, W.R., Thornton, J.M., 1992. The rapid generation of mutation data matrices from protein sequences. Comput. Appl. Biosci. 8, 275–282.

Kumar, S., Stecher, G., Li, M., Knyaz, C., Tamura, K., 2018. MEGA X: molecular evolutionary genetics analysis across computing platforms. Mol. Biol. Evol. 35, 1547–1549. https://doi.org/10.1093/molbev/msy096.

Lawrence, M.J., Wright, P.A., Wood, C.M., 2015. Physiological and molecular responses of the goldfish (*Carassius auratus*) kidney to metabolic acidosis, and potential mechanisms of renal ammonia transport. J. Exp. Biol. 218, 2124–2135. https://doi.org/10.1242/jeb.117689.

Liew, H.J., Sinha, A.K., Nawata, C.M., Blust, R., Wood, C.M., De Boeck, G., 2013. Differential responses in ammonia excretion, sodium fluxes and gill permeability explain different sensitivities to acute high environmental ammonia in three freshwater teleosts. Aquat. Toxicol. 126, 63–76. https://doi.org/10.1016/j.aquatox.2012.10.012.

López-González, Z., Ayala-Aguilera, C., Martinez-Morales, F., Galicia-Cruz, O., Salvador-Hernández, C., Pedraza-Chaverri, J., Medeiros, M., Hernández, A.M., Escobar, L.I., 2016. Immunolocalization of hyperpolarization-activated cationic HCN1 and HCN3 channels in the rat nephron: regulation of HCN3 by potassium diets. Histochem. Cell Biol. 145, 25–40. https://doi.org/10.1007/s00418-015-1375-6.

Nawata, C.M., Hung, C.C.Y., Tsui, T.K.N., Wilson, J.M., Wright, P.A., Wood, C.M., 2007. Ammonia excretion in rainbow trout (*Oncorhynchus mykiss*): evidence for Rh glycoprotein and H^+-ATPase involvement. Physiol. Genomics 31, 463–474. https://doi.org/10.1152/physiolgenomics.00061.2007.

Perry, S.F., Gilmour, K.M., 2006. Acid-base balance and CO_2 excretion in fish: unanswered questions and emerging models. Respir. Physiol. Neurobiol. 154, 199–215. https://doi.org/10.1016/j.resp.2006.04.010.

Rubino, J.G., Wilson, J.M., Wood, C.M., 2019. An in vitro analysis of intestinal ammonia transport in fasted and fed freshwater rainbow trout: roles of NKCC, K^+ channels, and Na^+, K^+ ATPase. J. Comp. Physiol. B. 189, 549–566. https://doi.org/10.1007/s00360-019-01231-x.

Santoro, B., Tibbs, G.R., 1990. The HCN gene family: molecular basis of the hyperpolarization-activated pacemaker channels. Ann. N. Y. Acad. Sci. 868, 741–764.

Sarbahi, D.S., 1951. Studies of the digestive tracts and the digestive enzymes of the goldfish, *Carassius auratus* (Linnaeus) and the largemouth black bass, *Micropterus salmoides* (Lacépède). Biol. Bull. 100, 244–257.

Shahi, P.K., Choi, S., Zuo, D.C., Kim, M.Y., Park, C.G., Kim, Y.D., Lee, J., Park, K.J., So, I., Jun, J.Y., 2014. The possible roles of hyperpolarization-activated cyclic nucleotide channels in regulating pacemaker activity in colonic interstitial cells of Cajal. J. Gastroenterol. 49, 1001–1010. https://doi.org/10.1007/s00535-013-0849-3.

Sinha, A.K., Liew, H.J., Diricx, M., Blust, R., De Boeck, G., 2012a. The interactive effects of ammonia exposure, nutritional status and exercise on metabolic and physiological responses in gold fish (*Carassius auratus* L.). Aquat. Toxicol. 109, 33–46. https://doi.org/10.1016/j.aquatox.2011.11.002.

Sinha, A.K., Liew, H.J., Diricx, M., Kumar, V., Darras, V.M., Blust, R., De Boeck, G., 2012b. Combined effects of high environmental ammonia, starvation and exercise on hormonal and ion-regulatory response in goldfish (*Carassius auratus* L.). Aquat. Toxicol. 114–115, 153–164. https://doi.org/10.1016/j.aquatox.2012.02.027.

Sinha, A.K., Liew, H.J., Nawata, C.M., Blust, R., Wood, C.M., De Boeck, G., 2013. Modulation of Rh glycoproteins, ammonia excretion and Na^+ fluxes in three freshwater teleosts when exposed chronically to high environmental ammonia. J. Exp. Biol. 216, 2917–2930. https://doi.org/10.1242/jeb.084574.

Skou, J.C., 1960. Further investigations on a mg^{++} + Na^+-activated adenosinetriphosphatase, possibly related to the active, linked transport of Na^+ and K^+ across the nerve membrane. Biochim. Biophys. Acta 42, 6–23.

Stevens, D.R., Seifert, R., Bufe, B., Müller, F., Kremmer, E., Gauss, R., Meyerhof, W., Kaupp, U.B., Lindemann, B., 2001. Hyperpolarization-activated channels HCN1 and HCN4 mediate responses to sour stimuli. Nature 413, 631–635. https://doi.org/10.1038/35098087.

Sutcliff, R.L., Li, S., Gilbert, M.J., Schulte, P.M., Miller, K.M., Farrell, A.P., 2020. A rapid intrinsic heart rate resetting response with thermal acclimation in rainbow trout, *Oncorhynchus mykiss*. J. Exp. Biol. Jeb. 215210. https://doi.org/10.1242/jeb.215210.

Towle, D.W., Holleland, T., 1987. Ammonium ion substitutes for K^+ in ATP-dependent Na^+ transport by basolateral membrane vesicles. Am. J. Phys. Regul. Integr. Comp. Phys. 252, R479–R489. https://doi.org/10.1152/ajpregu.1987.252.3.r479.

Tsui, T.K.N., Randall, D.J., Hanson, L., Farrell, A.P., Chew, S.F., Ip, Y.K., 2004. Dogmas and controversies in the handling of nitrogenous wastes: Ammonia tolerance in the oriental weatherloach *Misgurnus anguillicaudatus*. J. Exp. Biol. 207, 1977–1983. https://doi.org/10.1242/jeb.00905.

Turner, L.A., Bucking, C., 2017. The interactive effect of digesting a meal and thermal acclimation on maximal enzyme activities in the gill, kidney, and intestine of goldfish (*Carassius auratus*). J. Comp. Physiol. B Biochem. Syst. Environ. Physiol. 187, 959–972. https://doi.org/10.1007/s00360-017-1068-7.

Verdouw, H., Van Echteld, C.J.A., Dekkers, E.M.J., 1978. Ammonia determination based on indophenol formation with sodium salicylate. Water Res. 12, 399–402. https://doi.org/10.1016/0043-1354(78)90107-0.

Wilson, C.M., Stecyk, J.A.W., Couturier, C.S., Nilsson, G.E., Farrell, A.P., 2013. Phylogeny and effects of anoxia on hyperpolarization-activated cyclic nucleotide- gated channel gene expression in the heart of a primitive chordate, the Pacific hagfish (*Eptatretus stoutii*). J. Exp. Biol. 216, 4462–4472. https://doi.org/10.1242/jeb.094912.

Wood, C.M., 2019. Internal spatial and temporal CO_2 dynamics: Fasting, feeding, drinking, and the alkaline tide. In: Fish Physiology. Elsevier Inc, pp. 245–286. https://doi.org/10.1016/bs.fp.2019.07.003.

Wood, C.M., Bucking, C., Grosell, M., 2010. Acid-base responses to feeding and intestinal Cl^- uptake in freshwater- and seawater-acclimated killifish, *Fundulus heteroclitus*, an agastric euryhaline teleost. J. Exp. Biol. 213, 2681–2692. https://doi.org/10.1242/jeb.039164.

Wright, P.A., Wood, C.M., 2012. Seven things fish know about ammonia and we don't. Respir. Physiol. Neurobiol. 184, 231–240. https://doi.org/10.1016/j.resp.2012.07.003.

Zhang, L., Nawata, C.M., Wood, C.M., 2013. Sensitivity of ventilation and brain metabolism to ammonia exposure in rainbow trout, *Oncorhynchus mykiss*. J. Exp. Biol. 216, 4025–4037. https://doi.org/10.1242/jeb.087692.

Zhang, L., Nawata, C.M., De Boeck, G., Wood, C.M., 2015. Rh protein expression in branchial neuroepithelial cells, and the role of ammonia in ventilatory control in fish. Comp. Biochem. Physiol. Part A Mol. Integr. Physiol. 186, 39–51. https://doi.org/10.1016/j.cbpa.2014.10.004.

Zimmer, A.M., Nawata, C.M., Wood, C.M., 2010. Physiological and molecular analysis of the interactive effects of feeding and high environmental ammonia on branchial ammonia excretion and Na^+ uptake in freshwater rainbow trout. J. Comp. Physiol. B. 180, 1191–1204. https://doi.org/10.1007/s00360-010-0488-4.

Zong, X., Stieber, J., Ludwig, A., Hofmann, F., Biel, M., 2001. A single histidine residue determines the pH sensitivity of the pacemaker channel HCN2. J. Biol. Chem. 276, 6313–6319. https://doi.org/10.1074/jbc.M010326200.